

Optical-ellipsometric study of the nematic-to-smectic transition in 8CB films adsorbed on silicon

S. Chakraborty and R. Garcia

Department of Physics, Worcester Polytechnic Institute, Worcester, Massachusetts 01609, USA

(Received 20 September 2009; revised manuscript received 23 December 2009; published 4 March 2010)

The nematic-to-smectic-A (NA) transition in 8CB (4-octyl-4'-cyanobiphenyl) is especially interesting because experimentally, it has been observed to be second order, but theoretically, it has been predicted that it must have a latent heat. The effect on the NA transition due to confinement in an adsorbed film has hitherto not been investigated. Previous study of adsorbed 8CB films on silicon for coverages less than 100 nm showed the existence of a broad coexistence region, identified by the formation of thick and thin islands on the surface that extends between the bulk NA and the isotropic-to-nematic transition temperatures. In this paper, optical and ellipsometric measurements of 8CB films as a function of temperature are used to identify the location of the NA transition in the film in relation to the coexistence region. The NA transition temperature in the film is found to occur at 32.2 ± 0.4 °C independent of film thickness for films between 62 to 270 nm thick, based on the decrease in the film anisotropy. This decrease in the anisotropy is found to be surprisingly abrupt. For thicknesses below 62 nm, the NA transition line is joined to the thin-thick coexistence region found previously.

DOI: [10.1103/PhysRevE.81.031702](https://doi.org/10.1103/PhysRevE.81.031702)

PACS number(s): 42.70.Df, 61.30.Jf, 05.70.Jk

I. INTRODUCTION

The nematic-to-smectic-A (NA) transition in liquid crystals has been shown to share many features in common with the superfluid transition in ^4He and the normal to superconductor transition in high T_c superconductors [1,2]. Despite many advances, however, certain features of this transition remain poorly understood and even controversial [2]. Alternative theoretical models that have been proposed include the Halperin-Lubensky-Ma (HLM) theory of fluctuation-induced first-order transitions [3], the self-consistent one-loop theory of Patton and Andereck [4], the gauge transformation method of Lubensky and co-workers [5], and the dislocation unbinding (DLU) model of Nelson and co-workers [6].

A key feature in the theory of the NA transition is a coupling between the NA order parameter ψ and fluctuations in the director due to the isotropic-to-nematic (IN) transition, which typically occurs at a somewhat higher temperature [2]. For superconductors, the equivalent coupling is between ψ and the vector potential fluctuations. According to HLM, this coupling introduces a correction to the free energy $\sim \psi^3$ which drives the transition to first order [3]. Nevertheless, when the NA and IN transitions are far apart in temperature, this latent heat is expected to become unobservable. Thus, this model is not seen to necessarily contradict thermodynamic studies observing second-order specific heat peaks with XY universality class exponents [7,8]. Subsequently, there have been a number of attempts to derive the critical behavior of the NA transition for wide nematic ranges where the latent heat is negligible [4–6]. The DLU theory proposes that dislocations and dislocation loops play the role of vortices and vortex loops, respectively, in a superfluid or superconductor, and that the NA transition corresponds to the lowest temperature where the dislocations nucleate in the form of unbound pairs [6]. This theory remains controversial, however, because a key prediction is that the critical properties near the NA transition should exhibit inverted XY behavior [6], where “inverted” means the temperature axis is re-

versed relative to the location of T_{NA} , but experimentally measured specific heat data consistently show “noninverted” XY behavior [8].

As physical systems are shrunk to ever smaller dimensions, their actual properties increasingly deviate from their bulk properties, giving rise to a variety of finite-size phenomena. The prediction and observation of such phenomena in liquid crystals or simple fluids have been the subject of many studies [9–12]. Only recently have studies begun to look at how confinement in an adsorbed film geometry affect phase transitions in liquid crystalline films of 5CB (4-pentyl-4'-cyanobiphenyl) and 8CB (4-octyl-4'-cyanobiphenyl) adsorbed on silicon [13–15]. In both these films, a “coexistence region” is observed that extends downwards in temperature from T_{IN} . Within this coexistence region, thick and thin islands form and persist stably side by side on the surface. For 8CB films, this coexistence region extends from the bulk $T_{\text{IN}}=40.5$ °C down past the bulk $T_{\text{NA}}=33.6$ °C, for films thinner than ~ 60 nm. The location, however, of the NA transition in the film as a function of thickness has not been determined in those experiments [15].

Based on bulk properties of 8CB and considerations from HLM theory, the NA transition in 8CB films would be expected to continue to be characterized by negligible latent heat. For the nCB (n-alkyl-cyanobiphenyl) family of liquid crystals, the Landau tricritical point separating second-order and first-order behavior is identified experimentally to occur very close to 9CB (4-nonyl-4'-cyanobiphenyl), where the McMillan ratio $T_{\text{NA}}/T_{\text{IN}}=0.994$ [16]. For 8CB (4-octyl-4'-cyanobiphenyl), with $T_{\text{NA}}/T_{\text{IN}}=0.978$, the NA transition in the bulk is observed to be second order (or at least the latent heat is negligibly small) [7,8]. In addition, for an adsorbed 8CB film, previous experiments have established that homeotropically aligned smectic cybotactic partial bilayers [14] are preferentially formed at both the vapor and substrate interfaces even very far above the NA transition temperature, with smectic period of 3.2 nm [15,17,18]. Near the Si surface, however, a complex 4.1-nm-thick 8CB layer is first formed [15,17]. For these boundary conditions, the director fluctuations specifically responsible for the first-

order behavior would be expected to be further suppressed.

In this paper, spectroscopic ellipsometry is used to obtain the optical anisotropy and film thickness as a function of temperature for films ranging from 20 to 270 nm in thickness. From this data, we determine the location of NA transition as a function of film thickness and show the relation of the NA transition to the thin-thick coexistence region observed previously in 8CB. Separately, we also report micrographs of textures which accompany the transition in the film.

II. EXPERIMENT

A. Film preparation

The 8CB films with thicknesses in the range 20–300 nm as determined by ellipsometry, are prepared by spin coating dilute solutions of 8CB in chloroform which contains 1% ethanol as a stabilizer as described in Ref. [15]. The films as deposited at room temperature on 2 cm × 2 cm substrates are very smooth and uniform with thickness varying ± 2 nm in the middle 70% of the substrate. Due to the high vapor pressure, the solvent quickly evaporates over about a total of 30 s during spin casting, so the thickness of the films is controlled by varying the concentration of the 8CB solution and the acceleration of the programmable Laurel spin coater. Additional solvent is observed to degas from the film when heating from room temperature to 32 °C using our standard protocol. Reflection IR reveals no discernible sign of chloroform in the film by the time the ellipsometric data are taken, however, it is possible that some trace amounts of ethanol are present based on a weak reflectance peak at ~ 3600 cm^{-1} . Throughout the film preparation, the laboratory conditions are maintained at a temperature of about 27 °C and ambient humidity of about 40%, but these did not have a discernible effect on the prepared film thickness which is found to have completely smectic order, with a sharp x-ray Bragg peak at the smectic period of 3.2 nm [15].

B. Spectroscopic ellipsometry

The location of the NA transition was determined using spectroscopic ellipsometry, which provides the film thickness and dielectric constants as a function of wavelength for each temperature as the film is gradually heated. The computer-controlled Woollam M-2000X ellipsometer used has a covered optical-access heat stage, allowing the sample temperature to be controlled to within 0.1 °C, when a fixed angle of incidence of 70° is used. During each run, every 5 min, a half second spectroscopic measurement was taken and then the temperature was increased by 0.1 °C. This rate of temperature increase was found by Ref. [15] to be sufficiently slow to maintain quasistatic conditions as the temperature is increased. For the present experiments, we found decreasing the rate of temperature change by a factor of two or more had no discernible effect (within experimental scatter) on the transition temperatures obtained on increasing temperature.

For the measurements, a spot size of 0.1 mm is obtained using focusing probes. The optical effect of the windows and focusing lenses is corrected based on a multiangle system

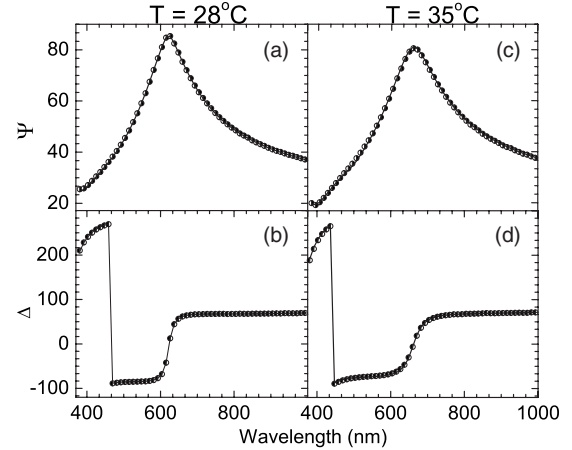


FIG. 1. Measured Stokes parameters Ψ and Δ in degrees of a typical film of thickness 131.3 ± 0.8 nm (a) below NA transition at 28 °C and (b) above NA transition at 35 °C. For clarity, only every other point is shown. The solid lines show the fits obtained using the single layer model described in the text. The shift from 270° to -90° in Δ seen at ~ 450 nm is due to the periodicity in the definition of the phase angle.

calibration provided by the COMPLETE-EASE software that came with the ellipsometer. The dc offset used to correct minor effects due to lamp aging and ambient lighting changes was determined before each run.

Prolonged exposure to the focused light beam with intensity of 6.33 mW/mm^2 [19] was observed to cause damage and/or thinning of the film at the point of incidence. This may have been because of some chemical reaction or localized heating of the film due to the intense light. In order to limit the exposure of the sample to the focused light, during each measurement, a normally closed shutter was opened for a total of only 1 s, including the time for the shutter to open and close. Exposure times of less than 2 s taking on point every 0.1 °C was determined to have no noticeable effect on the film or the data.

Figure 1 shows typical raw ellipsometric data (symbols) as a function of wavelength for a film of thickness 131.3 ± 0.8 nm, both above and below where the NA transition occurs in the film. The Stokes parameters Ψ and Δ are obtained from the ratio ρ of the total reflection coefficients parallel and perpendicular to the plane of incidence r_{pp} and r_{ss} , respectively, which are related via [20]

$$\rho = \frac{r_{pp}}{r_{ss}} = \tan(\Psi)e^{i\Delta}. \quad (1)$$

Consistent with the anisotropic nature of the liquid crystalline film, which is preferentially aligned along the vertical z direction, the off-diagonal reflection coefficients $r_{ps} = r_{sp} = 0$.

In order to extract information concerning film structure from Ψ and Δ , a model-dependent analysis of ellipsometric data is necessary. For the analysis, the simplest possible model is used where a single uniaxial dielectric film (liquid crystal) is assumed to sit atop a silicon substrate with a native oxide layer for which the dielectric constants have al-

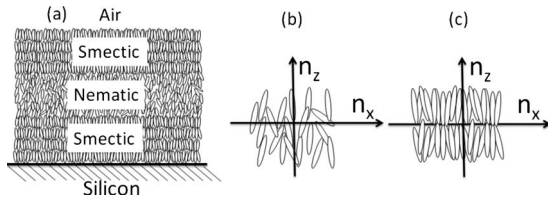


FIG. 2. Rough sketch (a) of expected ordering within the liquid crystalline film above the NA transition based on Refs. [15,17,18]. The ordering of 8CB molecules in the (b) nematic and (c) smectic A phases, showing why the anisotropy $\Delta n = n_z - n_x$ would be less in the nematic phase.

ready been determined [21]. The Fresnel equations for a single film on a substrate can then be used to calculate r_{pp} and r_{ss} [20]. For the fits, we use the COMPLETE-EASE 4.03 modeling package provided by JA Woollam Co., which specifically performs a simultaneous χ^2 minimization of the N , C , and S optical parameters that are calculated from the film thickness and complex optical constants as a function of wavelength as discussed in Ref. [20]. The optical constants parallel and perpendicular to the plane of incidence are independently modeled as a function of wavelength for each temperature using the B -spline technique described in Ref. [22]. In this technique, Kramers-Kronig consistency between the real and imaginary parts of the dielectric constants is strictly enforced. Since the dielectric film on top of the silicon is organic, optical transparency is assumed above a wavelength of 500 nm [19].

Figure 2(a) shows a putative, rough schematic of the expected structure of the adsorbed 8CB film on silicon above the NA transition temperature based on the results of Refs. [14,15,17,18] discussed in the introduction. Due to the non-uniform structure in the film above the NA transition, the optical constants obtained from fitting the ellipsometric data represent an average over the entire film. Because the disordered nematic phase has a lower anisotropy $\Delta n = n_z - n_x$ [compare Figs. 2(b) and 2(c)], we expect that Δn will decrease as the film enters the nematic phase.

III. RESULTS

A. Ellipsometry

Figure 3 shows Δn for a 120 nm film going up to 33 °C and then down in temperature. The significant hysteresis in Fig. 3 is surprising in more than one respect. To determine the temperature of the NA transition, we take the average of the extreme upper and lower limits of the sharp step in Δn , henceforth called “kinks.” We find that T_{NA} is 0.9 °C lower going down in temperature than going up. It is also surprising and significant that at *slower* temperature scan rate the hysteresis actually *increases*: on increasing the temperature, the step in Δn occurs at the same place, but the step occurs even lower upon decreasing the temperature and the mean square error (MSE) is more than three times higher. The hysteresis, which has not been observed in the bulk, rather than being due to a latent heat, may be explained instead in terms of a kind of “surface memory effect” [23] where sur-

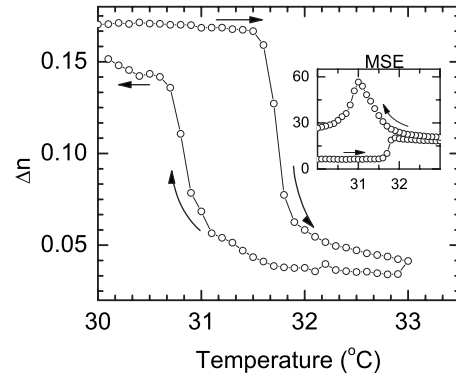


FIG. 3. Anisotropy Δn for a 120 nm film going up and then down in temperature, showing an even lower NA transition temperature when cooling from the nematic phase, possibly due to increased disorder in the film. Inset shows mean square error (MSE) in arb. units for the fit.

face textures formed at the vapor interface as we approach T_{NA} from above present a nonuniform surface on which the smectic phase nucleates; defect boundaries would then be expected where these domains later join together as the temperature is lowered further. To avoid such artifacts, subsequent data were taken only going up in temperature.

Figure 4 shows Δn and total thickness as a function of temperature for the data shown in Fig. 1, which was taken as the temperature is increased. Figure 4 contains the three most surprising outcomes of our analysis: first, the NA transition in the film is signaled by a sharp step in Δn approximately 0.4 °C wide, rather than by a smooth increase beginning at T_{NA} as would be expected in the bulk; second, the transition

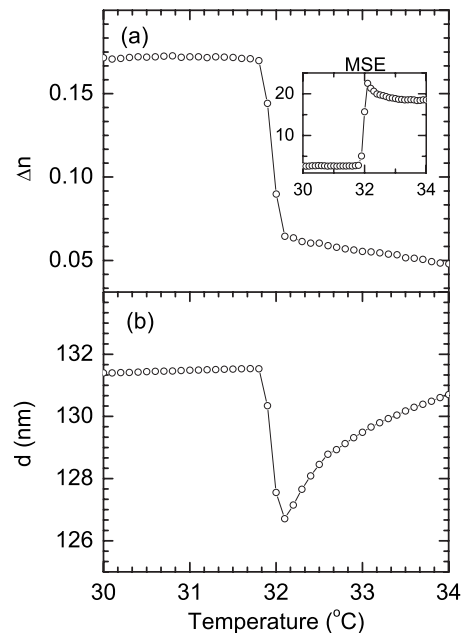


FIG. 4. Results of fitting the ellipsometric data for a film of 131 nm coverage (film thickness at room temperature) as the temperature is increased: (a) Δn at a wavelength of 632.8 nm, plotted as a function of temperature for the film in Fig. 1. (b) The total film thickness. The inset shows the MSE for the fit.

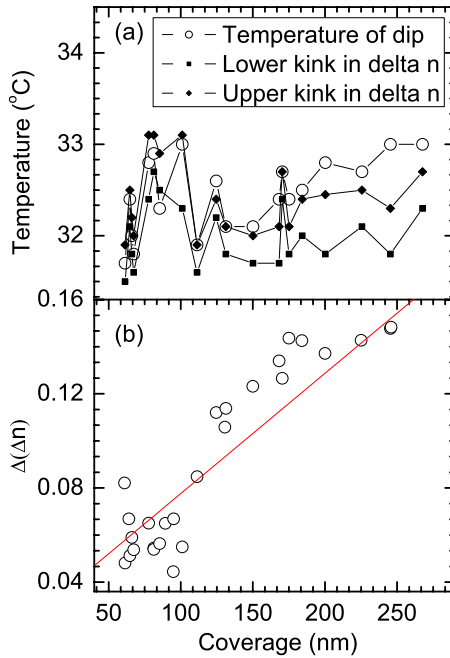


FIG. 5. (Color online) Summary of experimental results on heating for all coverages studied. (a) The temperatures of the upper and lower kinks in Δn and of the minimum of the dip in total thickness, plotted as a function of coverage. (b) The size of the step in Δn versus coverage.

temperature (taken to be the average of the upper and lower kinks in the sharp step in Δn) is ~ 1.4 °C below the bulk $T_{NA} = 33.6$ °C [24]; third, a narrow, asymmetric dip in the film thickness is observed to coincide closely with the T_{NA} of the film. It is possible that this dip in the thickness is an artifact produced by the rapidly changing dielectric constant, roughness, or other changes in the film structure that are not taken into account in the fit. In particular, while the step in Δn appeared to be independent of the temperature scan rate, the dip in the thickness became somewhat larger and more asymmetric for slower scan rates. Nevertheless, it is always present both on heating and cooling and associated closely with the step in Δn .

The extreme upper and lower limits of the step in Δn , which we refer to as kinks, are easily discerned from the data, although in general, there is an observable degree of rounding present. Figure 5(a) shows the temperature of the upper and lower kink in Δn as well as the location of the minimum of the dip in the total thickness on heating, for all of the films as a function of surface coverage (film thickness at room temperature). Large scatter is evident in the data, which on the whole are consistent with T_{NA} of 32.2 ± 0.4 °C, that is independent of film thickness, but 1.4 °C lower than the bulk transition temperature, as confirmed for our sample by calorimetry [24]. For films thinner than 110 nm, the minimum in the thickness occurs between the upper and lower kinks of the step in Δn , but for thicker films the minimum occurs as much as 0.4 °C above. Figure 5(b) shows that the size of the step in Δn increases linearly with the coverage.

The lowered T_{NA} does not appear to be due to residual solvent left from the film preparation. Reflection IR reveals

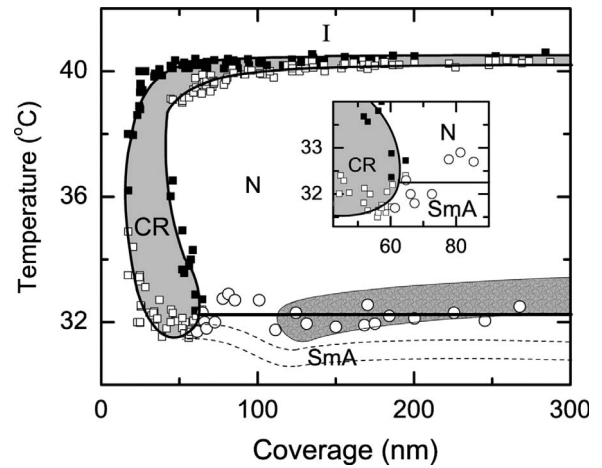


FIG. 6. Phase diagram indicating the thin-thick coexistence region CR (shaded area bounded by dark lines) and the NA transition determined by the average of the temperatures of the upper and lower kink in the jump in Δn (open circles with best fitted line). The isotropic, nematic, and smectic A regions are labeled as I, N, and SmA. The two dashed lines about a degree below the NA transition and immediately below the coexistence region indicate the approximate temperatures when dark streaks and patches show on the surface (Fig. 7). The light shaded region straddling the NA transition line for coverages above 120 nm are where surface textures are observed on the surface (Fig. 8).

that the broad peak due to ethanol at ~ 3600 cm^{-1} decreases significantly if we heat the film for a twice as long on the heat stage, presumably due to degassing of residual ethanol. However, the transition temperature obtained upon heating does not change measurably.

B. Microscopy

In addition to ellipsometric measurements, optical microscopy was used to observe the surface of the film near the NA transition temperature and to establish the relationship of the NA transition occurring in the film to the thin-thick coexistence region first described in Ref. [15].

Figure 6 shows a phase diagram summarizing all the new optical and ellipsometric results. This phase diagram extends the result of Ref. [15] to a maximum thickness of 270 nm. The coexistence region (CR) was identified, as in Ref. [15], by the appearance of dark and light islands on the surface, or alternatively, via an accompanying signature in ellipsometric data. Overall, the boundaries of the coexistence region as determined by the new experiments are shifted to lower thickness by 6 ± 2 nm. A possible explanation for this discrepancy is that the new film thicknesses are obtained directly from *in situ* ellipsometric measurements, whereas those of Ref. [15] were determined based on an *ex situ* x-ray calibration. In addition, plotted on the diagram are the NA transition temperatures as described above. It is to be noted that on the scale of the phase diagram, it would be very difficult to distinguish the various points indicated in Fig. 5. The solid line marking the NA transition in the film was found to join the thin-thick coexistence region at a thickness of 63 ± 2 nm.



FIG. 7. (Color online) Dark patches that appear on the surface of a film of coverage 95 nm 0.5°C below the film T_{NA} . Similar patches are observed for all coverages $0.4\text{--}1.0^\circ\text{C}$ below the film T_{NA} . The illuminated area in the image is 1.5 mm across.

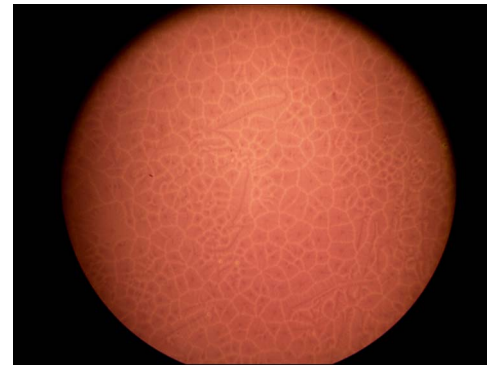
The two dashed lines $0.4\text{--}1.0^\circ\text{C}$ below the NA transition and immediately below the coexistence region indicate the temperatures when dark streaks and narrow patches show on the surface (shown in Fig. 7). These streaks may be related to the structural reorganization within the film before the transition actually occurs, but do not seem to coincide with any obvious signature in the ellipsometry data.

Figure 6, also shows a region surrounding the NA transition temperature where further interesting textures are observed on the surface for films thicker than 120 nm. Figure 8 shows micrographs of these surface textures for films of thickness 135 and 270 nm. The textures first form just below or right at the NA transition in the film and persist for as much as 1.2°C above. Since they are observed through fine changes in the reflected color, they are observed with greater or lesser clarity depending on the precise thickness of the films. As the temperature is increased first, wrinkles or cracks appear throughout the film. With increasing temperature, these cracks further spread apart so that we are left with what appear to be islands or chunks floating in a liquid. As the temperature is increased yet further, the contrast between these two regions diminishes and then the textures disappear altogether.

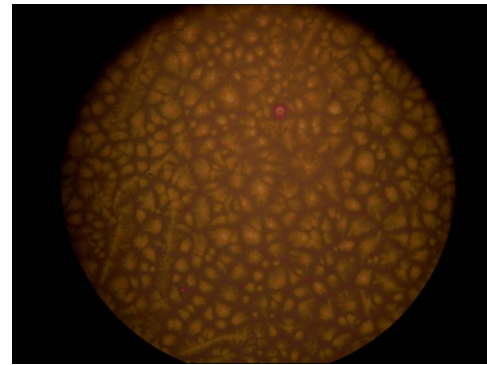
IV. DISCUSSION

According to HLM, the coupling of nematic and smectic order parameters causes the NA transition to always be first order. Our measurements of 8CB films are unique because the homeotropic boundary conditions imposed by the vapor and substrate [14,15,17,18] would be expected to quench the very fluctuations in the director within the film that are responsible for the predicted first-order character of the NA transition according to HLM theory [3].

The hysteresis observed in the data (Fig. 3), the presence of a sharp jump in the order parameter [Fig. 4(a)], and the large scatter in T_{NA} (Fig. 5) could be taken as an evidence of first-order character, confirming the HLM theory. However, many aspects of the data are equally consistent with the DLU theory of the NA transition [6]. For example, the observed hysteresis is very large (~ 1 K) and odd since only the T_{NA} on cooling changes with scan rate. Normally, for a first-order



(a)



(b)

FIG. 8. (Color online) Micrographs of films showing surface textures that are found to be closely associated with the NA transition for coverages greater than 120 nm, and which persist up to 1.2°C above the film T_{NA} . The illuminated area in each image is 1.5 mm across. The upper micrograph is for a 135 nm film at 0.1°C below T_{NA} , whereas the lower one is for a 270 nm film at 0.4°C above T_{NA} .

transition with metastable regions, we would expect the hysteresis to *decrease* with lower scan rate. At the same time, such a strange and asymmetric hysteresis may be explained by surface memory effects associated with textures at the vapor interface (as noted in the description of Fig. 3). And a sharp jump in the order parameter is also expected for a second-order Kosterlitz-Thouless (dislocation unbinding) transition [25]. The increase in the size of the step in Δn with coverage shown in Fig. 5 indicates that thicker films possess a greater degree of disorder in the nematic phase than thinner films. For sufficiently thick films, where boundary effects are negligible, the difference in Δn between nematic and smectic phases would be expected to saturate at a certain value. The fact that the increase in Δn with coverage is found to be linear [Fig. 5(b)] may be an indication that the films studied are sufficiently thin that the boundaries have a limiting effect. Further investigation is necessary to establish whether the dip in thickness [Fig. 4(b)] is or is not an artifact. Nevertheless, the presence of a dip also would be consistent with the DLU theory, since it could potentially be explained as the effect of fluctuation-induced Casimir force associated with the dislocation loop fluctuations [10,12,15,26].

For films thicker than 120 nm, interesting surface textures (Fig. 8) were observed to form just below the NA transition in the film and persist for as much as a degree above. These textures at the very least indicate that at T_{NA} , there is more going on in the film than merely a uniform nematic layer intruding between two smectic layers as function of height as depicted in Fig. 2. Similar looking textures have been predicted above the NA transition, due to isolated smectic islands within a wider nematic phase [2]. While textures may correspond to such islands, we do not think the evolution of these regions as a function of temperature entirely fits this interpretation, because the regions between the round textures do not grow with temperature, but rather gradually merge with the round features until they are indistinguishable. Thus, the pattern appears to us to be more consistent with what is expected from the DLU model where the proliferation of dislocation loops causes the NA transition. A horizontal dislocation loop has the form of an additional layer of layers which intrude between a given set of smectic layers, causing the film thickness to pop up where the extra layers intrude [6]. In addition, there is no reason why we should not expect a contribution due to dislocation loops at an angle with respect to the horizontal as well as vertical dislocation pairs. These would be expected to pierce the surface and cause a variation in the order parameter horizontally as well as vertically within the film. We do not at present know how to model such variation in the ellipsometric data and therefore cannot possibly hypothesize what are the phases in the micrographs presented in Fig. 8.

V. CONCLUSIONS

In these experiments, the temperature of the NA transition in films between 20 to 270 nm thick was determined in relation to the thick-thin coexistence region that had been observed previously [15]. We observed four surprising phenomena that accompany the transition: first, a sharp step rather than a smooth increase in Δn beginning at T_{NA} ; second, a transition temperature that is suppressed 1.4 °C below the bulk T_{NA} ; third, a narrow, asymmetric dip in the film thickness that coincides closely with the transition, which

may or may not be an artifact; fourth, a pronounced hysteresis on going up and down in temperature. We also observed textures which appear on the surface of the film close to T_{NA} , which indicate that more is going on in the film than can be described by a smooth variation in the order parameter with height depicted in Fig. 2 and assumed by many theoretical models of what happens in films [10,13–15,17].

We were not able to conclusively interpret these surprising results either in the context of the many somewhat contradictory theories of the NA transition [1–4,6] or solely on the basis of our own experimental data. Possible explanations for the significant depression of T_{NA} in the film may be finite-size effects, trapped defects, stresses, or gradients within the film due to the imposed vapor and substrate boundary conditions. Attempts to reduce the amount of residual solvent in the film did not measurably affect the transition temperature, but there still may have been some solvent present even after these measures. There are also multiple possible explanations of the observed hysteretic behavior (Fig. 3) and the step in Δn [Fig. 4(a)] that are potentially consistent with the HLM view of the NA transition [3] being first order as well the DLU view of the transition being a kind of second-order Kosterlitz-Thouless unbinding transition [6]. Given the magnitude of the hysteresis in the film and its relative total absence in the bulk, it would be useful to study the size of the hysteresis to see if it decreases for even thicker films. To establish whether dip in the film thickness [Fig. 4(b)] is due to a fluctuation-induced force [10,12,15,26] or due to other causes, improvement in the temperature resolution and a method of calibrating the magnitude of the force are needed.

ACKNOWLEDGMENTS

This research was supported by NSF under Grant No. DMR 0821292 and ACS PRF under Grant No. 45840-G5. We also acknowledge extremely beneficial discussions with James Hilfiker and Jeffrey S. Hale at J. A. Woollam Inc. We also thank Germano S. Iannacchione, Satyendra Kumar, Eftim Milkani, John C. McDonald, Tom C. Lubensky, Masafumi Fukuto, Abhik Mukhopadhyay, and Krishna Sigdel for fruitful comments.

-
- [1] K. Kobayashi, J. Phys. Soc. Jpn. **29**, 101 (1970); W. L. Mc-Millan, Phys. Rev. A **4**, 1238 (1971).
- [2] A. DeVries, Mol. Cryst. Liq. Cryst. **10**, 31 (1970); **10**, 219 (1970); **11**, 361 (1970); P. G. de Gennes, Solid State Commun. **10**, 753 (1972); Mol. Cryst. Liq. Cryst. **21**, 49 (1973); P. G. de Gennes and J. Prost, *The Physics of Liquid Crystals*, 2nd ed. (Clarendon, Oxford, 1993).
- [3] B. I. Halperin, T. C. Lubensky, and Shang-keng Ma, Phys. Rev. Lett. **32**, 292 (1974); M. A. Anisimov, P. E. Cladis, E. E. Gorodetskii, D. A. Huse, V. E. Podneks, V. G. Taratuta, W. van Saarloos, and V. P. Voronov, Phys. Rev. A **41**, 6749 (1990).
- [4] B. R. Patton and B. S. Andereck, Phys. Rev. Lett. **69**, 1556 (1992); B. S. Andereck and B. R. Patton, Phys. Rev. E **49**, 1393 (1994).
- [5] T. C. Lubensky and Jing-Huey Chen, Phys. Rev. B **17**, 366 (1978); T. C. Lubensky and J. De Chim, J. Chim. Phys. Physicochim Biol. **80**, 31 (1983); T. C. Lubensky and A. J. McKane, Phys. Rev. A **29**, 317 (1984).
- [6] D. R. Nelson and J. Toner, Phys. Rev. B **24**, 363 (1981); C. Dasgupta and B. I. Halperin, Phys. Rev. Lett. **47**, 1556 (1981); J. Toner, Phys. Rev. B **26**, 462 (1982).
- [7] J. Thoen, H. Marynissen, and W. Van Dael, Phys. Rev. A **26**, 2886 (1982); E. Anesta, G. S. Iannacchione, and C. W. Garland, Phys. Rev. E **70**, 041703 (2004); Andrzej Żywociński and Stefan A. Wiczorek, J. Phys. Chem. B **101**, 6970 (1997).
- [8] C. W. Garland, G. Nounesis, and K. J. Stine, Phys. Rev. A **39**,

- 4919 (1989); C. W. Garland, G. Nounesis, K. J. Stine, and G. Heppke, *J. Phys. (Paris)* **50**, 2291 (1989); P. Das, G. Nounesis, C. W. Garland, G. Sigaud, and N. H. Tinh, *Liq. Cryst.* **7**, 883 (1990); G. Nounesis, C. W. Garland, and R. Shashidhar, *Phys. Rev. A* **43**, 1849 (1991); C. W. Garland, M. Meichle, B. M. Ocko, A. R. Kortan, C. R. Safinya, L. J. Yu, J. D. Litster, and R. J. Birgeneau, *ibid.* **27**, 3234 (1983); C. W. Garland, G. Nounesis, M. J. Young, and R. J. Birgeneau, *Phys. Rev. E* **47**, 1918 (1993); C. W. Garland and G. Nounesis, *ibid.* **49**, 2964 (1994).
- [9] John D. Reppy, *J. Low Temp. Phys.* **87**, 205 (1992); M. H. W. Chan, K. I. Blum, S. Q. Murphy, G. K. S. Wong, and J. D. Reppy, *Phys. Rev. Lett.* **61**, 1950 (1988); G. S. Iannacchione, C. W. Garland, J. T. Mang, and T. P. Rieker, *Phys. Rev. E* **58**, 5966 (1998).
- [10] M. E. Fisher and P. G. de Gennes, *C. R. Acad. Sci. (Paris) Ser. B* **287**, 207 (1978); A. Ganshin, S. Scheidmantel, R. Garcia, and M. H. W. Chan, *Phys. Rev. Lett.* **97**, 075301 (2006); M. Fukuto, Y. F. Yano, and P. S. Pershan, *ibid.* **94**, 135702 (2005); A. Hucht, *ibid.* **99**, 185301 (2007); A. Maciotek, A. Gambassi, and S. Dietrich, *Phys. Rev. E* **76**, 031124 (2007); R. Zandi, A. Shackell, J. Rudnick, M. Kardar and L. P. Chayes, *ibid.* **76**, 030601(R) (2007).
- [11] Charles Rosenblatt, Ronald Pindak, Noel A. Clark, and Robert B. Meyer, *Phys. Rev. Lett.* **42**, 1220 (1979); J. D. Litster, *Phys. Today* **35** (5), 25 (1982).
- [12] Gary A. Williams, *Phys. Rev. Lett.* **92**, 197003 (2004); *Physica C* **404**, 415 (2004); B. Markun and S. Zumer, *Phys. Rev. E* **73**, 031702 (2006).
- [13] D. van Effenterre, R. Ober, M. P. Valignat, and A. M. Cazabat, *Phys. Rev. Lett.* **87**, 125701 (2001); D. van Effenterre and M. P. Valignat, *Eur. Phys. J. E* **12**, 367 (2003); P. Ziherl and S. Zumer, *ibid.* **12**, 373 (2003); S. Schlagowski, K. Jacobs, and S. Herminghaus, *Europhys. Lett.* **57**, 519 (2002); F. Vandembrouck, M. P. Valignat, and A. M. Cazabat, *Phys. Rev. Lett.* **82**, 2693 (1999); D. van Effenterre, M. P. Valignat, and D. Roux, *Europhys. Lett.* **62**, 526 (2003).
- [14] P. Ziherl and S. Zumer, *Eur. Phys. J. E* **12**, 361 (2003); P. Ziherl, R. Podgornik, and S. Zumer, *Phys. Rev. Lett.* **84**, 1228 (2000); P. Ziherl, F. Karimi Pour Haddadan, R. Podgornik, and S. Zumer, *Phys. Rev. E* **61**, 5361 (2000).
- [15] R. Garcia, E. Subashi, and M. Fukuto, *Phys. Rev. Lett.* **100**, 197801 (2008); Z. M. A. Ewiss, G. Nabil, S. Schlagowski, and S. Herminghaus, *Liq. Cryst.* **31**, 557 (2004).
- [16] J. Thoen, H. Marynissen, and W. Van Dael, *Phys. Rev. Lett.* **52**, 204 (1984); B. M. Ocko, R. J. Birgeneau, J. D. Litster, and M. E. Neubert, *ibid.* **52**, 208 (1984).
- [17] L. Xu, M. Salmeron, and S. Bardon, *Phys. Rev. Lett.* **84**, 1519 (2000).
- [18] M. Fukuto, O. Gang, K. J. Alvine, B. M. Ocko, and P. S. Pershan, *Phys. Rev. E* **77**, 031607 (2008).
- [19] James Hilfiker (private communication).
- [20] G. E. Jellison, Jr., *Thin Solid Films* **290-291**, 40 (1996); H. G. Tompkins and W. A. McGahan, *Spectroscopic Ellipsometry and Reflectometry* (Wiley, New York, 1999), cf. pp. 220–224.
- [21] C. M. Herzinger *et al.*, *J. Appl. Phys.* **83**, 3323 (1998).
- [22] B. Johs and J. S. Hale, *Phys. Status Solidi A* **205**, 715 (2008).
- [23] N. A. Clark, *Phys. Rev. Lett.* **55**, 292 (1985).
- [24] Krishna Sigdel and G. S. Iannacchione (private communication).
- [25] J. M. Kosterlitz and D. J. Thouless, *J. Phys. C* **6**, 1181 (1973); B. I. Halperin and D. R. Nelson, *Phys. Rev. Lett.* **41**, 121 (1978); **41**, 519 (1978); D. J. Bishop and J. D. Reppy, *ibid.* **40**, 1727 (1978); D. R. Nelson and B. I. Halperin, *Phys. Rev. B* **19**, 2457 (1979); P. M. Chaikin and T. C. Lubensky, *Principles of Condensed Matter Physics* (Cambridge University Press, Cambridge, England, 1995).
- [26] X. S. Chen and V. Dohm, *Phys. Rev. E* **70**, 056136 (2004).